Supporting Information

Layer-Controlled CVD Growth of Large-Area Two-Dimensional MoS_2 Films

Jaeho Jeon[a], Sung Kyu Jang[a], Su Min Jeon[a], Gwangwe Yoo[b], Jin-Hong Park[b], and Sungjoo Lee[a,b,c]**

[a] SKKU Advanced Institute of Nanotechnology (SAINT), Sungkyunkwan University (SKKU), Suwon 440-746, Korea.

[b] School of Electronics and Electrical Engineering, Sungkyunkwan University, Suwon 440-746, Korea.

[c] Center for Human Interface Nanotechnology (HINT), Sungkyunkwan University (SKKU), Suwon 440-746, Korea.

*Corresponding Authors: jhpark9@skku.edu and leesj@skku.edu

Surface Treatment

Before the LPCVD process, 300 nm thick SiO_2/Si substrates were cleaned with acetone, IPA, and DI water with 15 min ultra-sonication and treated with oxygen plasma by using RIE equipment at 60 W and with 5 sccm O_2. The effects of the oxygen plasma treatments on the SiO_2 surfaces were examined with XPS (X-ray photoelectron spectroscopy) and by performing contact angle measurements. We examined the effects of the oxygen plasma on the SiO_2 surfaces with XPS. Figures S1a and b show the O1s XPS spectra of a bare SiO_2 substrate (Figure S1a) and of a SiO_2 substrate treated with oxygen plasma for 300 s (Figure S1b).

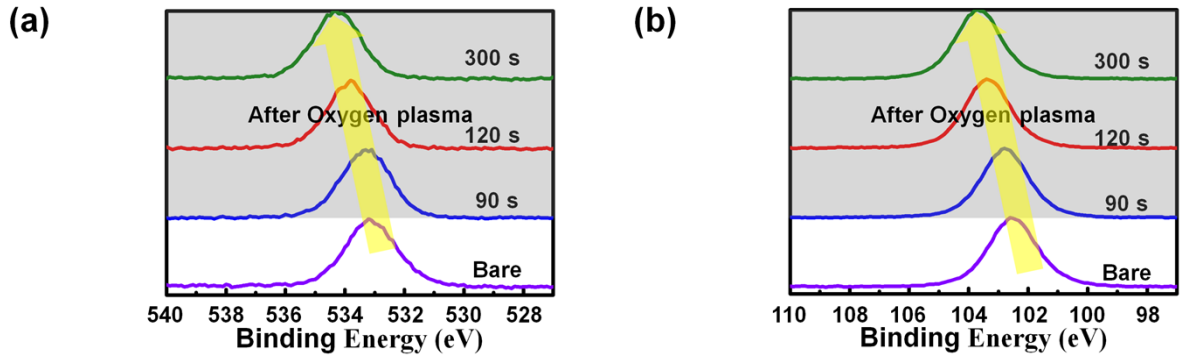

Figure S1. XPS measurement with different surface treatment conditions on SiO_2/Si substrate : (a) Si 2p XPS spectra with bare, 90 , 120, 300 sec oxygen plasma treatment on SiO_2 surface, (b) O 1s XPS spectra with bate, 90, 120, 300 sec oxygen plasma treatment on SiO_2 surface.

Figure S2 shows images of water droplets on the bare and treated substrates. The contact angle on the bare SiO_2 substrate is 24.5º (Figure S2a), whereas contact angles less than 1º were found for the plasma-treated SiO_2 substrates (Figures S2b, c, and d), which shows that the SiO_2 substrates become more hydrophilic as the plasma-treatment time increases.

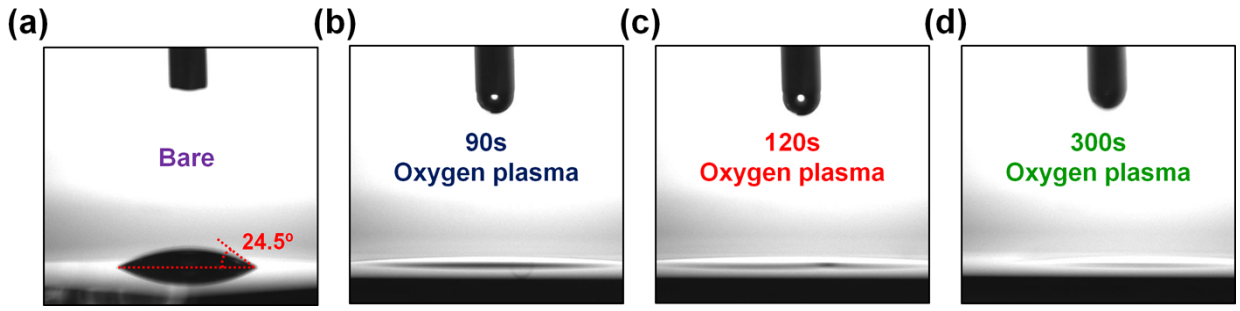

Figure S2. Images of water droplets on SiO_2/Si substrates. (a) Bare SiO_2, and after plasma treatments of various durations: (b) 90 s, (c) 120 s, and (d) 300 s.

Low Pressure CVD synthesis tool

The growth of the MoS_2 films was carried out in a LPCVD furnace, as shown in Figure S3a. Before the synthesis, MoO_3 powder was placed in the center of the heating zone and sulfur powder was placed 30 cm away from the MoO_3 powder. When the temperature of the CVD system reaches 850 ºC, the temperatures of the MoO_3 and sulfur positions rise to 790 ºC and 210 ºC, respectively (Figure S3b).

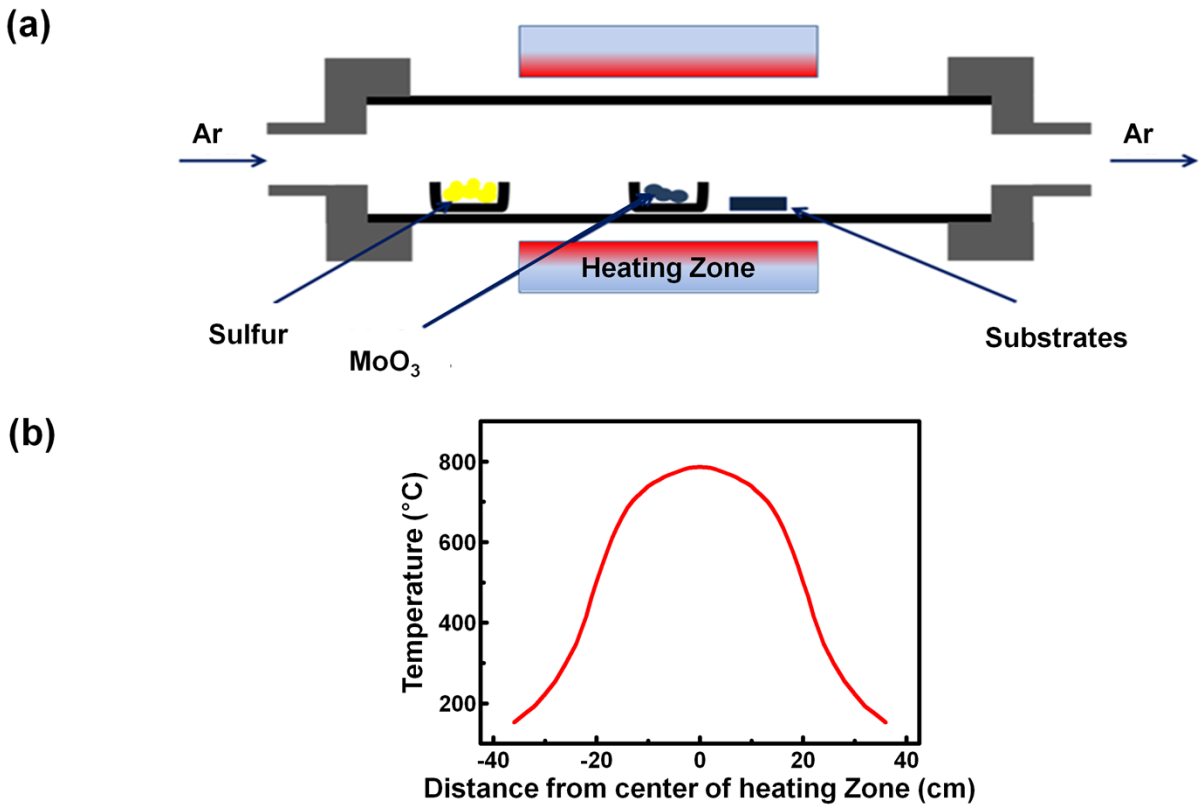

Figure S3. (a) Schematic diagram of the MoS_2 CVD growth system. (b) Variation of the temperature inside the quartz tube with the distance from the center of the heating zone.

Comparison of MoS_2 films grown on bare and plasma-treated SiO_2 substrates

Figure S4 shows SEM images of MoS_2 films grown on a bare SiO_2 substrate (a) and a SiO_2 substrate treated with oxygen plasma for 90 s (b). In the SEM images, the bright white areas are the SiO_2 substrates and the dark black areas are MoS_2. In (a), small triangular discontinuous MoS_2 grains are evident, whereas in (b) a continuous full-coverage MoS_2 film is present. Figures S4c and d show the Raman and PL spectra of these samples. The differences between the A^1_g and E^1_{2g} peak centers are the same (19.6 cm^{-1} ~ 20.6 cm^{-1}) for both samples, indicating that monolayer MoS_2 films are present on both substrates. However, the MoS_2 on the plasma-treated substrate exhibits much higher Raman and PL intensities.

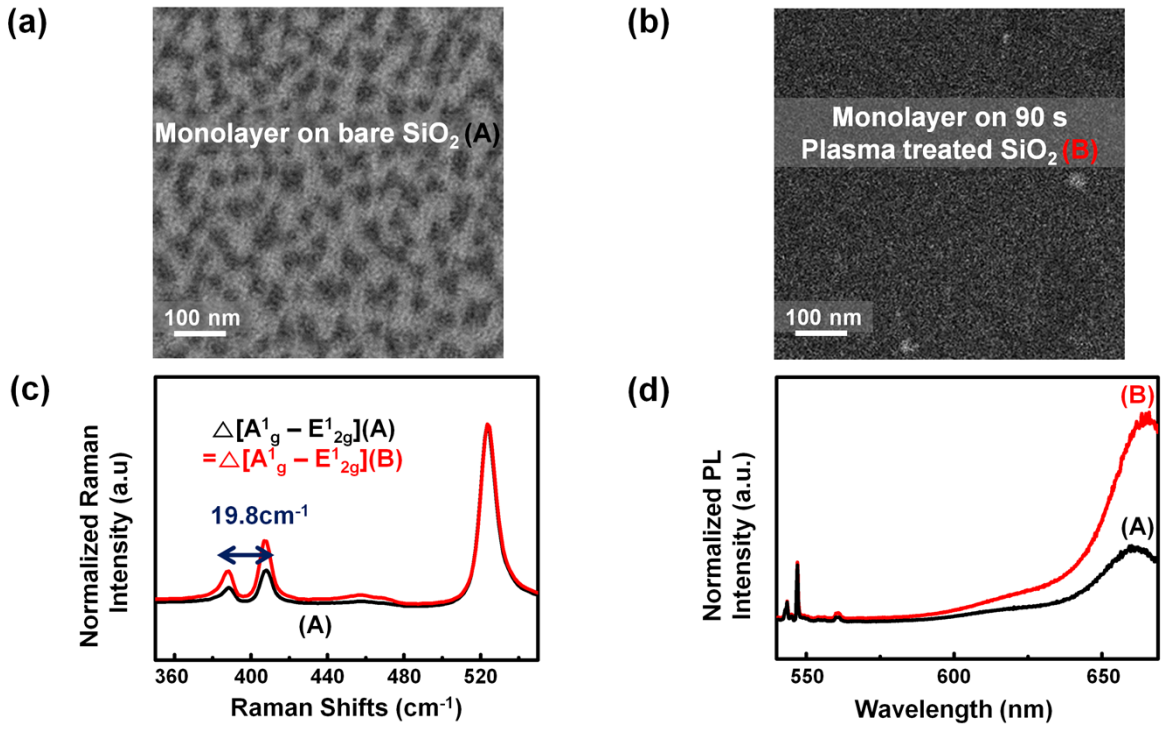

Figure S4. (a) SEM image of MoS_2 grown on a bare SiO_2 substrate. (b) SEM image of MoS_2 grown on a SiO_2 substrate treated with oxygen plasma for 90 s. (c) Raman measurements for the A^1_g and E^1_{2g} peaks of (a) and (b). (d) PL measurements for (a) and (b).

Chemical configuration

The chemical configurations of the MoS_2 films were studied by performing XPS analysis. In theory, MoS_2 can have two different lattice structures. One thermodynamically stable form of MoS_2 is the trigonal prismatic 2-H structure in which each molybdenum atom is prismatically coordinated by six surrounding sulfur atoms; the 1-T structure of MoS_2 is reached by a phase transition in which the coordination of the Mo atoms becomes octahedral. These two forms of MoS_2 have different properties: 2-H MoS_2 exhibits semiconducting behavior and 1-T MoS_2 is metallic.[1, 2] Figures S4a and b show the Mo 3d and S 2p spectra of a monolayer MoS_2 film. The Mo 3d peak positions are at binding energies of 229 and 232 eV and the S 2p peak positions are at binding energies of 161.8 and 162.9 eV, which are due to a 2H-MoS_2 crystal structure with Mo $3d_{5/2}$ and $3d_{3/2}$ orbitals and S $2p_{1/2}$ and $2p_{3/2}$ orbitals respectively.[3] These measurements match the characteristic band spectral positions of perfectly synthesized 2H-MoS_2 layers.[3] In addition, similar Mo 3d spectra (Figure S5c) and S 2p spectra (Figure S5d) were obtained for the trilayer MoS_2 film, which indicates that the trilayer MoS_2 film also has a 2-H crystal structure.

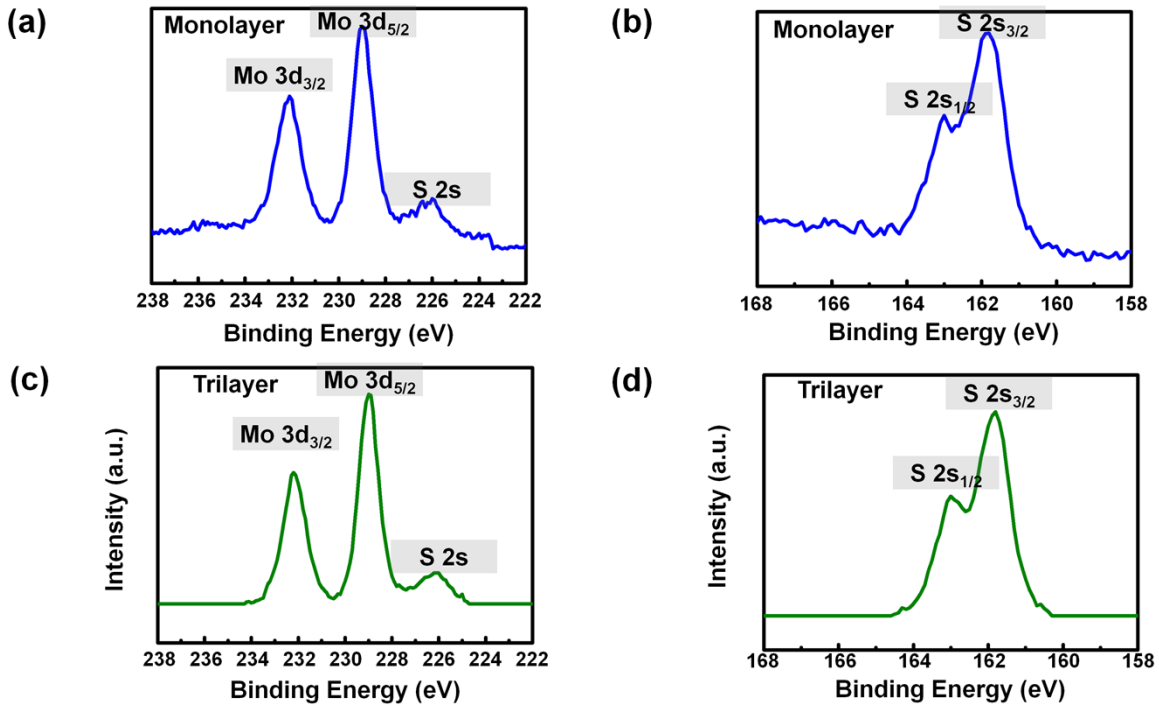

Figure S5. (a) Mo 3d and (b) S 2d XPS spectra for a monolayer MoS_2 film. (c) Mo 3d and (d) S 2d XPS spectra for a trilayer MoS_2 film.

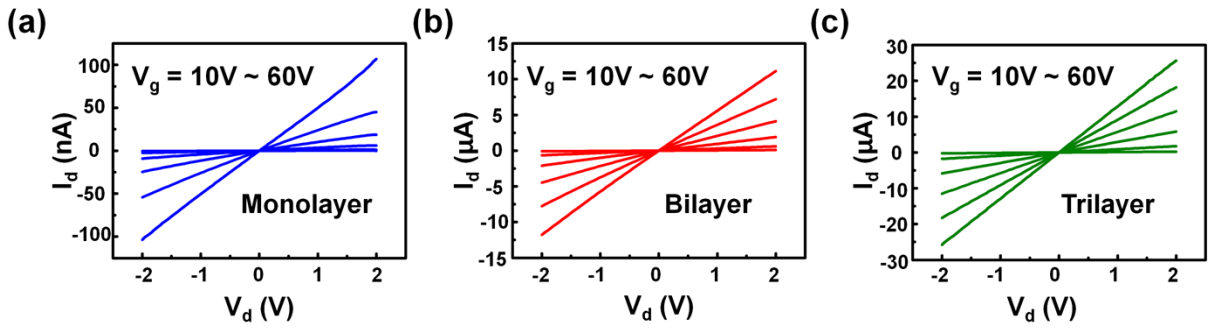

Figure S6. MoS_2 FET $I_d - V_d$ curves at various V_g (10 V ~ 60 V) for (a) monolayer MoS_2, (b) bilayer MoS_2, and (c) trilayer MoS_2.

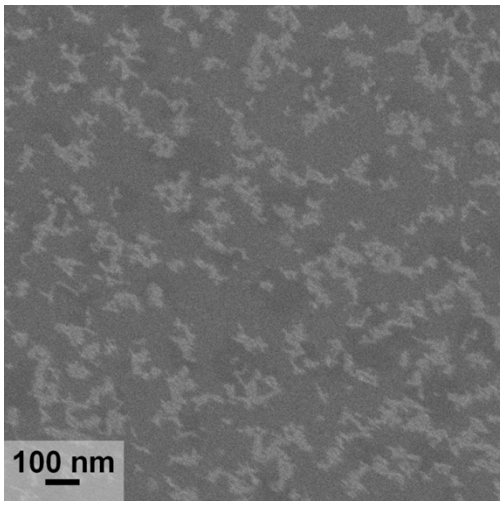

Figure S7. SEM image of the CVD-grown MoS_2 film on the 30 s oxygen plasma treated SiO_2 surface.

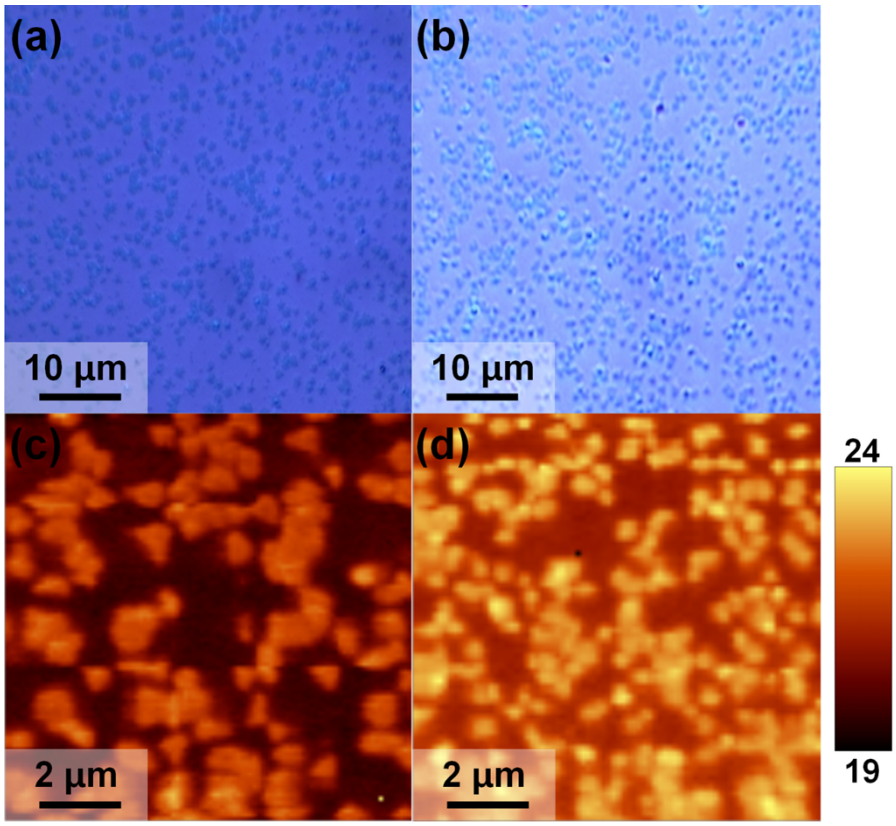

Figure S8. OM images of the CVD-grown MoS_2 films on the (a) 100 s and (b) 180 s oxygen plasma treated SiO_2 surface, and corresponding Raman mapping images of the CVD-grown MoS_2 films on the (C) 100 s and (d) 180 s oxygen plasma treated SiO_2 surface

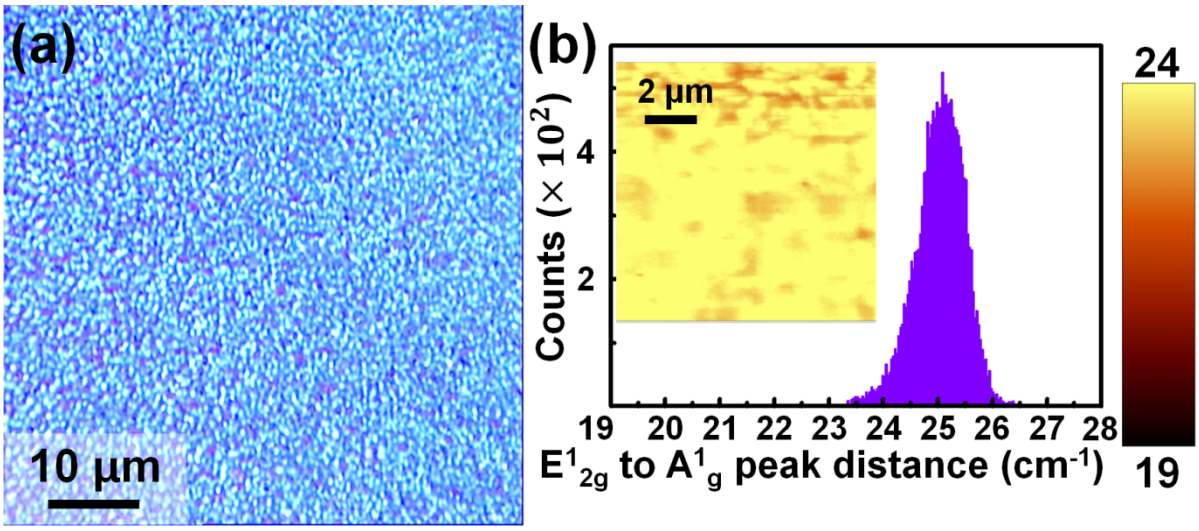

Figure S9. (a) OM image of the CVD-grown MoS_2 film on the 450 s oxygen plasma treated SiO_2 surface. (b) Statistical histogram of the E^1_{2g} to A^1_g peak distances and corresponding Raman mapping image of the CVD-grown MoS_2 film on the 450 s oxygen plasma treated SiO_2 surface.

REFERENCES

1 C. Ataca, H. Sahin, S. Ciraci, J Phys Chem C 2012, 116, 8983-8999.

2 C. A. Papageorgopoulos, W. Jaegermann, Surf Sci 1995, 338, 83-93.

3 G. Eda, H. Yamaguchi, D. Voiry, T. Fujita, M. W. Chen, M. Chhowalla, Nano Lett 2011, 11, 5111-5116.